Catalysis Today xxx (xxxx) xxx–xxx

Contents lists available at ScienceDirect

Catalysis Today

journal homepage: www.elsevier.com/locate/cattod

Vapor phase hydrogenolysis of glycerol to 1,2-propanediol at atmospheric pressure over copper catalysts supported on mesoporous alumina

M.L. Dieuzeide[a], R. de Urtiaga[a], M. Jobbagy[b], N. Amadeo[a,*]

[a] ITHES (UBA-CONICET), Laboratorio de Procesos Catalíticos, Departamento de Ingeniería Química, Facultad de Ingeniería, Universidad de Buenos Aires, Ciudad Universitaria, Pabellón de Industrias, 1428, Ciudad Autónoma de Buenos Aires, Argentina

[b] INQUIMAE (UBA-CONICET) Facultad de Ciencias Exactas y Naturales, Ciudad Universitaria, 1428, Ciudad Autónoma de Buenos Aires, Argentina

ARTICLE INFO

Keywords:
1,2-propanediol
Glycerol
Hydrogenolysis
CuO catalysts
Mesoporous alumina.

ABSTRACT

The present work explores the hydrogenolysis of glycerol to produce 1,2-propanediol in vapor phase at atmospheric pressure over copper catalysts supported on mesoporous alumina. Catalysts were prepared by alumina impregnation varying CuO loading between 3 wt% and 30 wt%. The textural and structural characteristics of the catalysts were determined by N_2 sorptometry (BET), powder X-ray diffraction (PXRD), temperature programmed reduction (TPR) and N_2O chemisorption (copper metallic area). The characterization showed that all catalysts present textural properties characteristic of mesoporous solids, such as the adsorption isotherms which are type IV. Based both on characterization and activity results, it was possible to conclude that the yield to 1,2-propanediol presented a non-monotonic dependence on total copper metallic area. In addition, it was proved that 1,2-propanediol production is associated with the presence of highly dispersed CuO phase in the solids. Promising results were obtained with CuO(15)Al catalysts, taking into account that the performance can be improved by increasing residence time.

1. Introduction

During the last decade biodiesel has gained attention as a biofuel, in particular because it can replace significant fractions of petroleum-derived fuels, both for stationary and mobile applications. Its production has markedly increased worldwide in the last decade with a forecast production for 2020 of 36.9 million metric tons [1]; in Argentina, one of the world major biodiesel producers, biodiesel production in 2014 reached 2.50 million tons [2].

Biodiesel is mainly produced by transesterification of oils and fats, being glycerol the main by-product (10 wt% of production). Consequently, glycerol has become a low cost building block, with high potential to be transformed into chemicals of high added value [2,3]. Among them, the production of 1,2-propanediol (1,2-PDO) by glycerol hydrogenolysis is of great interest due to the renewable character of this route. Traditionally, 1,2-PDO is produced by hydration of propylene oxide or ethylene oxide derived from propylene or ethylene, respectively [4].

Some applications for 1,2-PDO are in unsaturated polyester resins, as functional fluids such as anti-freezing and de-icing, in pharmaceutical products, food, cosmetics, liquid detergents, humectants for tobacco, flavorings and scents, personal hygienic products and paints [4]. In particular, the market of anti-freezing and de-icing products derived from 1,2-PDO is growing, as a consequence of the concern over the toxicity of ethylene glycol [5].

In the presence of a metallic catalyst and hydrogen, depending mainly on the reaction conditions and on the characteristics of the catalysts, glycerol can be converted into 1,2-PDO, 1,3-propanediol and ethylene glycol [6,7].

It is widely accepted that when the hydrogenolysis of glycerol is performed in vapor phase the reaction pathway is the dehydration − hydrogenation through an intermediate reactive which is acetol. In the first stage glycerol is dehydrated to form the intermediate, acetol. The second stage, reversible and exothermic, involves the hydrogenation of the intermediate to form finally 1,2-PDO [8–10].

The production of 1,2-PDO by glycerol hydrogenolysis employs catalysts mainly based on noble metals such as Pt, Ru, Pd, and Rh, or based on transition metals like Cu, Ni, or Co [4–6,8,11–17], regardless if the reaction is performed in liquid or vapor phase. In contrast to catalysts based on novel metals, that present lower selectivity to 1,2-PDO as consequence of the cleavage of the bond C−C [4,17–20]; catalysts based on copper offer both high conversions of glycerol and high selectivity to 1,2-PDO [4,15,21].

Different catalyst supports have been proposed for the

* Corresponding author.
E-mail address: norma@di.fcen.uba.ar (N. Amadeo).

http://dx.doi.org/10.1016/j.cattod.2017.05.095
Received 16 January 2017; Received in revised form 5 May 2017; Accepted 30 May 2017

hydrogenolysis of glycerol, some of them are Al_2O_3 [8,14,15,18,22–25]; SiO_2 [9,10,13,26,27]; ZnO/Al_2O_3, ZnO/TiO_2, ZnO/ZrO_2 [13,28], ZnO [29] and MgO [16]. The role of the support on the hydrogenolysis of glycerol to 1,2-PDO has been extensively discussed. Some authors have proposed that the acid or basic character of the support determine the reaction mechanism, when the reaction is carried out in liquid phase, and affects 1,2-PDO selectivity [4,6,17]. On the other hand, it has been proposed that, when the reaction is performed in vapor phase, metal-support interactions must be considered and the support has an important role in promoting the dispersion of the metallic phase [4]. In fact, in a previous study of our group it was proved that Al_2O_3 has no activity in vapor phase hydrogenolysis of glycerol [25].

Considering, as mentioned before, that the catalyst support has a great influence on the metal-support interaction as well as on metal dispersion [4], we have considered employing mesoporous alumina as support for copper based catalysts. Yuan et al. [30] proposed a facile synthesis of highly ordered mesoporous alumina with high thermal stability and tunable pore size by self-assembly of Pluronic 123, $(EO)_{20}(PO)_{70}(EO)_{20}$, triblock copolymer and alumina precursors in ethanolic solutions in the presence of additives such as nitric acid. This synthesis was then extended to obtain mesoporous alumina-supported noble metals or metal oxides [31–34]. Nevertheless there are few studies considering the impregnation of CuO over mesoporous alumina [35,36], these studies concluded that the textural and structural characteristic of mesoporous alumina have great influence both on copper metallic dispersion and on copper-support interactions.

Therefore, the aim of the present work is to analyse the effect of copper loading on catalytic activity in the hydrogenolysis of glycerol in vapor phase at atmospheric pressure, and its correlation with metallic copper dispersion.

2. Experimental

2.1. Catalyst preparation

Mesoporous alumina was prepared following a similar procedure to that reported by Yuan et al. [30] and Morris et al. [31]. For this synthesis, 25 g of $(EO)_{20}(PO)_{70}(EO)_{20}$ (Pluronic 123 of Sigma Aldrich) triblock copolymer were dissolved in 100 mL of anhydrous ethanol (99.5% Cicarelli). Then, 50 g of aluminum isopropoxide (98% Sigma Aldrich) were dissolved in 40 mL of nitric acid (65 v/v% Cicarelli) and 460 mL of ethanol. Once both solutions were dissolved they were combined, employing additionally 20 mL of ethanol, in order to transfer the solution of aluminum isopropoxide. The combined solution was kept under stirring for 24 h. Solvent evaporation was done at 60 °C for 48 h under air without stirring. Finally mesoporous alumina was obtained after calcining the precursor at 600 °C for 5 h.

Copper impregnation was performed by incipient wetness impregnation method with aqueous solutions of $Cu(NO_3)_2{\cdot}3H_2O$ (99.5% Merck), with concentrations ranging between 0.06 M and 6.3 M. Previously to impregnation, mesoporous alumina was ground and sieved, in order to obtain particles with diameters between 44 μm < dp < 88 μm. After impregnation with copper solutions, samples were dried at 120 °C for 6 h and then calcined at 400 °C for another 6 h. Both drying and calcination of impregnated samples were carried on in a stove under air atmosphere, with a temperature ramp of 10 °C/min. Fresh alumina is denoted as m-Al_2O_3 and the catalysts were denoted as: CuO(x)Al, being x the nominal CuO (wt%) loading, between 3 wt% and 30 wt%.

2.2. Catalyst characterization

Catalysts were characterized by several techniques.

Textural characterization was performed by N_2 sorptometry in a Micromeritics equipment ASAP 2020, employing 20 mg of sample.

Characterization by powder X-ray diffraction (PXRD) was performed with Siemens D5000 equipment, employing Cu Kα radiation.

Temperature programmed reduction (TPR) of fresh samples (after calcination) were performed in a Micromeritics Autochem II 2920, with a thermic conductivity detector (TCD). The samples (100 mg) were placed in a quartz U-shaped reactor. Previously to temperature programmed reduction, samples were pre-treated under a flow of Ar (50 mL/min) at 200 °C for 1 h. TPR was performed from 50 °C to 800 °C at a heating rate of 10 °C/min, under a flow of 100 mL/min of a mixture 2%H_2/Ar. Hydrogen consumption was determined by a TCD detector.

The dissociative N_2O adsorption method was performed in a Micromeritics Autochem II 2920 in order to determine copper metallic area and dispersion. The catalysts sample (100 mg) was placed in a U-shaped quartz reactor and was pre-treated in flowing Ar (50 mL/min) at 100 °C for 30 min, followed by cooling at room temperature. The catalyst pre-reduction, was performed increasing the temperature to 500 °C with a ramp of 10 °C/min under a 2% H_2/Ar (100 mL/min) flow for 30 min. Then the sample was cooled to 50 ± 5 °C in Ar flow (50 mL/min) and sequentially was exposed to a 50% N_2O/Ar flow (100 mL/min) for 1 h, in order to oxidize the Cu° to Cu_2O by dissociative adsorption of N_2O. Finally, after the purge of the sample under Ar flow (50 mL/min) at 50 °C for 15 min, the TPR was carried out, in order to reduce the Cu_2O species to metallic copper. This stage was performed in a 2% H_2/Ar flow (100 mL/min) and temperature was increased to 500 °C with a 10 °C/min ramp. The copper metallic area and dispersion, were calculated based on bibliography [37,38], considering that the number of superficial copper atoms per unit surface area is 1.47×10^{19} atoms/m^2 and the density of copper is 8.92 g/cm^3.

2.3. Catalytic activity

The hydrogenolysis of glycerol was carried out at atmospheric pressure in a stainless-steel continuous flow fixed bed reactor (Ø = 12 mm) placed in an electric furnace equipped with temperature controllers. Reaction temperature was measured with a k-type thermocouple, placed in the middle of the catalytic bed. For all catalytic tests, the liquid stream was fed with an HPLC bomb (Eldex 1HM) and vaporized in the initial third of the reactor. The liquid stream consisted of a water glycerol solution with a molar ratio ($R = n_{H_2O}/n_{C_3H_8O_3}$) R = 9:1 (35 wt% glycerol); with a liquid feed rate of 2.4 mL/h. The catalytic runs were performed isothermally at 240 °C, 0.5 g of catalyst were employed. Catalyst was diluted within an inert material in a ratio 1:5, in order to avoid temperature gradients. The hydrogen-glycerol molar ratio was 65:1. The feed stream was completed with Ar, as carrier. Both hydrogen and argon were fed to the reaction system by mass flow controllers (Brooks 0254), being the gaseous feed rate 360 mL/min.

The total flow rate and particle diameter were chosen in order to guarantee the absence of diffusional resistance during reaction tests.

Catalysts are reduced in situ at 500 °C (heating ramp of 10 °C/min) under a flow of 50% H_2/Ar (100 mL) during 30 min and under a flow of pure hydrogen (100 mL) for another 30 min. Then the catalytic bed temperature was set at reaction temperature (240 °C) under an Ar flow.

Both liquid feed samples and condensed samples were analysed by a GC (Agilent Technologies 7890A, DB-5, 30 m × 0.320 mm × 0.5 μm). Liquid samples were collected every hour during reaction. The internal standard method was used for the quantification of the results, being *n*-butanol the standard. The liquid products analysed were: 1,2-propanediol (propylene glycol), 1,3-propanediol, ethylene glycol and hydroxyacetone (acetol); no propanol was detected in the condensed stream. Gas stream was analysed by a GC (Agilent Tecnologies 6890N, Carboxen™ 1010 Plot, 30 m × 0.53 mm), however no gaseous products were detected except for non-reacted hydrogen. Since hydrogen is in excess respect to glycerol, it was not possible to estimate its consumption by chromatography.

In order to analyse the catalytic results, the following parameters were considered:

Table 1
BET surface area and pore volume for mesoporous alumina (m-Al_2O_3) and CuO(x)Al catalysts with x = 3–30 wt%. Chemisorption results: metallic area and dispersion of CuO (x)Al catalysts.

	BET Area (m^2/g)	Pore Volume (cm^3/g)	Metallic Area ($m^2/g_{catalysts}$)	Metallic Area (m^2/g_{Cu})	D (%)
m-Al_2O_3	243	0.66			
CuO(3)Al	272	0.50	3.2	107.3	16.6
CuO(5)Al	237	0.45	4.7	94.2	14.6
CuO(7)Al	266	0.38	5.7	80.9	12.5
CuO(10)Al	175	0.33	6.9	69.8	10.8
CuO(15)Al	137	0.21	10.0	67.0	10.4
CuO(20)Al	146	0.13	12.7	63.3	9.8
CuO(25)Al	97	0.16	14.6	58.3	9.1
CuO(30)Al	76	0.14	15.3	51.0	7.9

- Glycerol conversion: $x_G = \frac{[molesofglycerol]_{in} - [molesofglycerol]_{out}}{[molesofglycerol]_{in}} 100$
- Yield: $Y_i = \frac{[molesofoneproduct]_{out}}{[molesofglycerol]_{in}} 100$

The catalytic tests took 6 h under reaction conditions. In addition, carbon balance in all experiments was 100 ± 5%.

3. Results and discussion

3.1. Characterization results

Textural characterization results of mesoporous alumina and CuO (x)Al catalysts are shown in Table 1. The BET surface areas of catalysts with low copper loading (minor or equal to 7 wt%) are similar to the BET surface area of mesoporous alumina, this result indicates that mesoporous structure remains accesible in a wide range of copper contents. Catalysts with CuO loading between 10 wt% and 20 wt%, have BET surface areas around 150 m^2/g; while for high CuO loadings (25 wt% and 30 wt%) the BET surface areas are below 100 m^2/g. The pore volume decreases as copper loading increases. These results suggest that some pore blockage might have occurred with increasing copper loading.

The adsorption-desorption isotherms corresponding to mesoporous alumina and some catalyst are shown in Fig. 1. All of them, independently of copper loading, behave in terms of a type IV isotherms; which are characteristics of mesoporous solids. The hysteresis loop of the adsorption-desorption isotherm of the alumina is H1, indicating that the prepared alumina has a relatively high pore size uniformity and facile pore connectivity [39]. However as copper loading increases the hysteresis loops of the adsorption-desorption isotherms become H3. According to Kruk and Jaroniec [39] these types of hysteresis loop had been associated to solids comprised of aggregates of platelike particles forming slitlike pores; or could be indicative of the presence of disordered domains resulting from collapse of lamellar structure [40].

The PXRD patterns of mesoporous alumina and CuO(x)Al catalysts are presented in Fig. 2. Well-defined diffraction peaks neither could be detected in PXRD pattern of m-Al_2O_3, nor in samples with CuO loading equal or lower than 20 wt%. Diffraction peaks associated with CuO tenorite phase (2θ = 35.5°, 38.8°) are observed on the PXRD pattern of CuO(25)Al and CuO(30)Al catalysts indicating incipient bulk-CuO segregation. No signal of $CuAl_2O_4$ phases was observed.

The PXRD patterns corresponding to reduced catalysts are shown in Fig. 3. Diffraction peaks associated to metallic copper were not observed for loadings equal or lower than 20 wt%. This result, in agreement with PXRD patterns corresponding to fresh catalysts, suggests high metallic copper dispersion. For catalysts with CuO loadings of 25 wt% and 30 wt%, diffraction peaks associated to metallic copper were observed at 2θ = 43.5°; 53.1° and 74.1°.

The TPR profiles for CuO(x)Al catalysts are presented in Fig. 1. The maximum reduction temperature shifts to lower temperatures as copper loading increases, indicating that high copper loadings results in weaker copper support interactions. From the TPR profiles three reduction events of copper can be distinguished: at temperatures higher than 450 °C copper aluminate reduction takes place [23,35][23,35,0]; at temperatures between 300 and 450 °C the reduction of dispersed CuO with strong interaction with the alumina occurs, highly dispersed copper [34,35,40] and bulk-CuO which reduces at temperatures around 260 °C [23,41,42]. For catalysts with low copper loadings no segregation of bulk-CuO phase could be detected. The reduction events for catalysts with CuO loading between 7 wt% and 20 wt%, indicates that the main copper phase is copper with high interaction with alumina. The TPR profiles of catalysts with CuO content equal or higher than 15 wt%, present a shoulder that become the main peak with higher copper content at a temperature around 260 °C. This reduction event is associated to the reduction of bulk-CuO to metallic Cu [23,41,42]. For CuO loadings of 25 wt% and 30 wt% a reduction event associated to the reduction of copper phases similar to $CuAl_2O_4$ is observed. Since no diffraction peak corresponding to $CuAl_2O_4$ phases are distinguished in PXRD patterns corresponding to the reduced sample it is possible to suppose that the formation copper phases similar to $CuAl_2O_4$ occurred during the TPR runs where samples were subjected to temperatures higher than that of calcination. The formation of this kind of phases could be due to the fact that copper diffuses into alumina, acquiring a spinel type environment.

The TPR profiles are in accordance with PXRD patterns, since only for the highest copper loadings it was possible to distinguished diffraction peaks associated to the segregation of CuO phase.

The results of N_2O chemisorption are shown in Table 1. The metallic area per gram of catalyst increased with copper loading. Instead

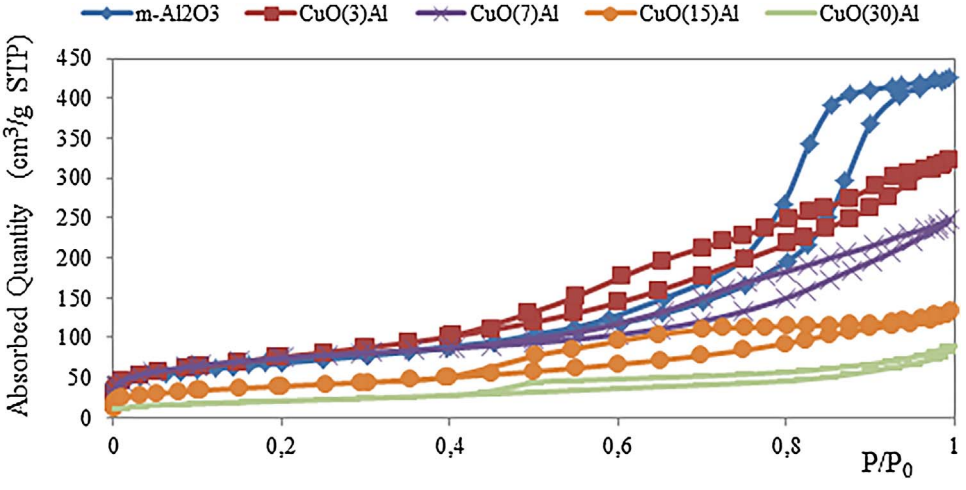

Fig. 1. Nitrogen adsorption-desorption isotherm of mesoporous alumina and some CuO(x)Al catalysts.

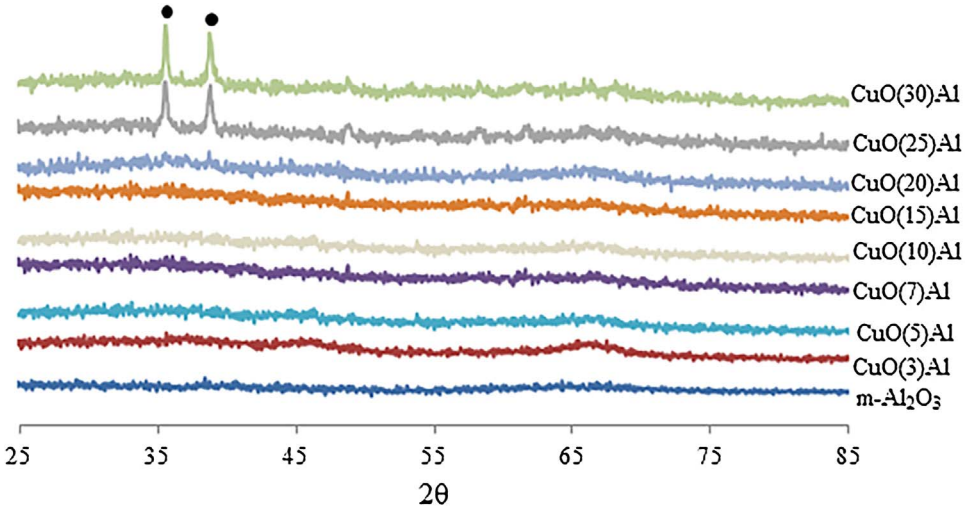

Fig. 2. PXRD patterns of mesoporous alumina and fresh CuO(x)Al catalysts. (●) Bulk-CuO (PDF- 45-0937).

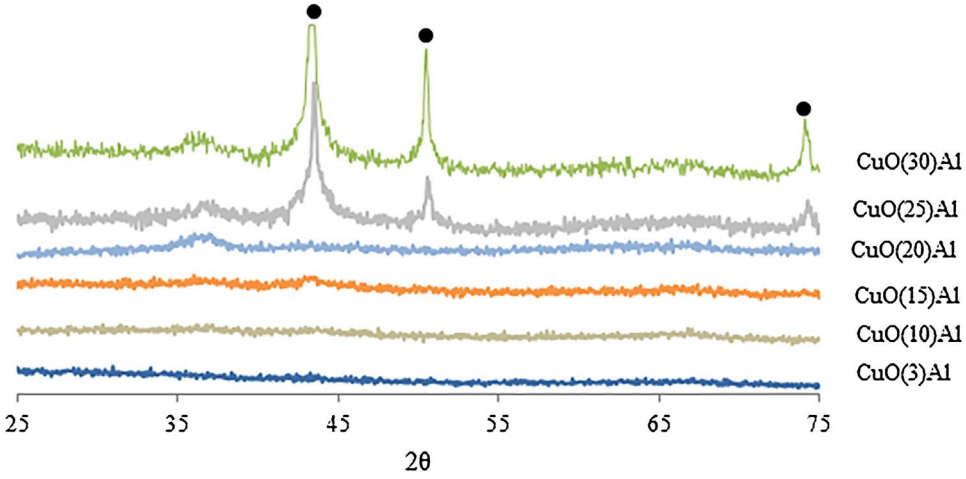

Fig. 3. PXRD patterns of reduced CuO(x)Al catalysts. (●) Metallic copper (PDF-04-0836).

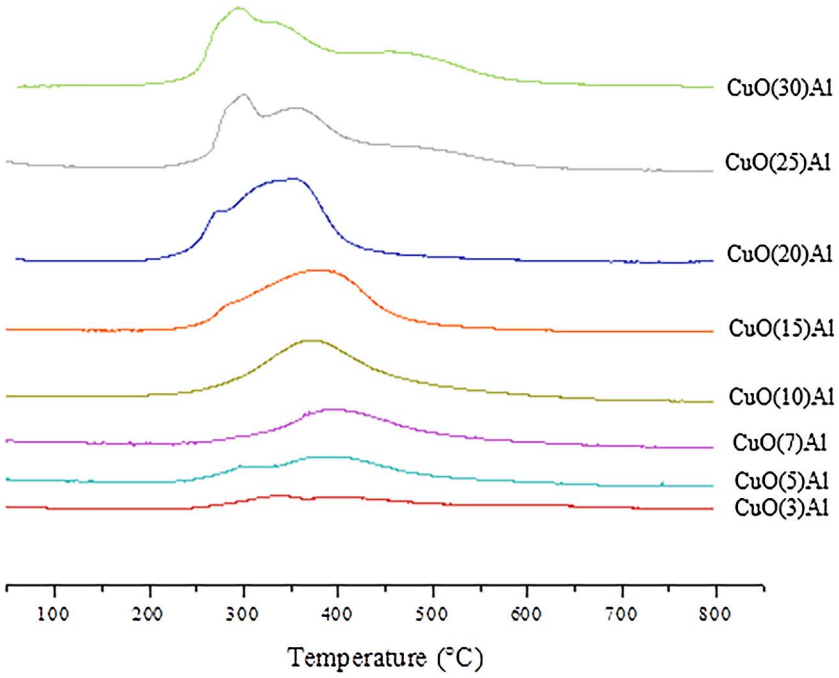

Fig. 4. TPR profiles of CuO(x)Al catalysts.

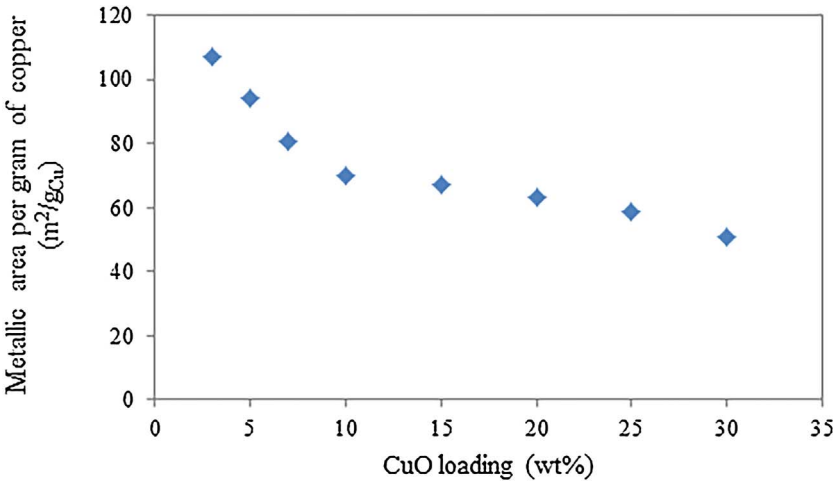

Fig. 5. Metallic area per gram of copper for CuO(x)Al catalysts.

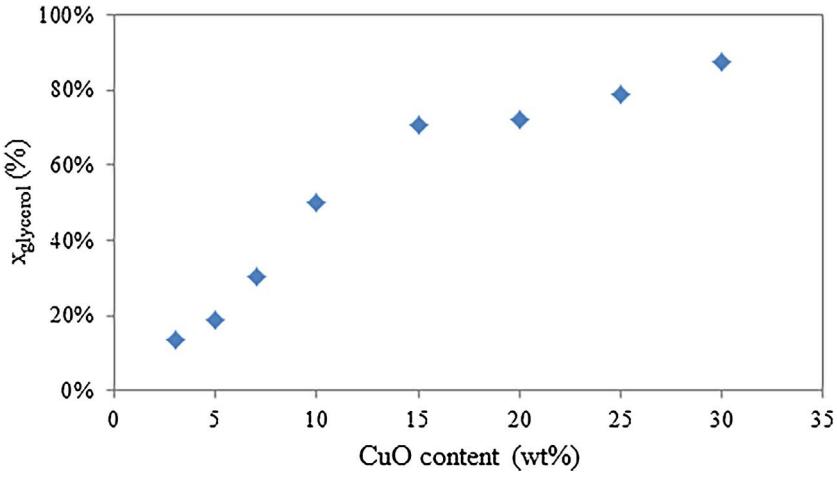

Fig. 6. Glycerol conversion vs. CuO content for CuO(x)Al catalysts.

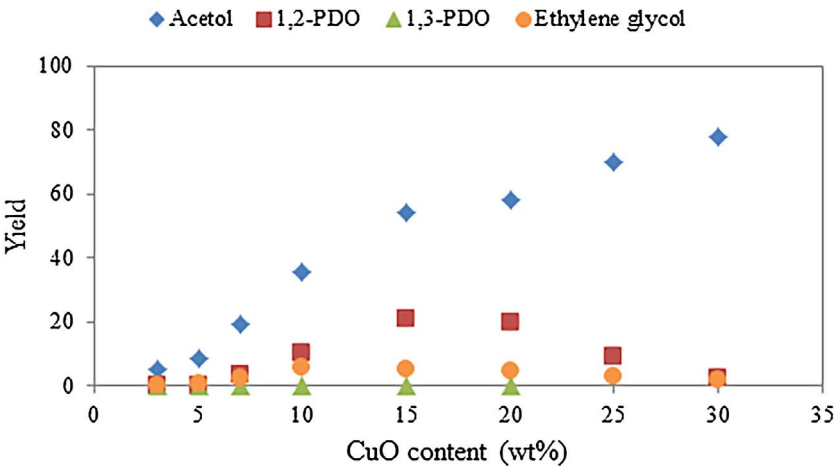

Fig. 7. Yield to acetol, 1,2-propanediol, 1,3-propanediol and ethylenglycol vs. CuO content for CuO(x)Al catalysts.

metallic area per gram of copper and metallic dispersion diminished with copper loading. The dispersion values are in agreement with the PXRD patterns and TPR profiles, since the higher dispersion values were obtained for those catalysts in which copper has strong interaction with the support. The metallic surface area per gram of copper as a function of loading is shown in Fig. 5. The metallic surface per gram of copper decreases linearly, with copper loading. However it is important to note that the slope changes between 10 wt% and 15 wt%. This change in the slope of metallic area per gram of copper agrees with the segregation of bulk-CuO phase detected by TPR. The diminishing metallic area per gram of copper at low CuO loadings (equal or lower than 10 wt%), could be explained by the formation of copper phases with decreasing interaction with the support in agreement with the low reduction temperature observed in the corresponding TPR profiles. For catalysts with high CuO loadings (equal or higher than 15 wt%), the diminishing metallic area per gram of copper could be attributed to the growth of CuO particles, as it has been concluded in PXRD patterns for catalysts with CuO loadings of 25 wt% and 30 wt%.

3.2. Activity results

Glycerol conversion increased with loading, as shown in Fig. 6. The

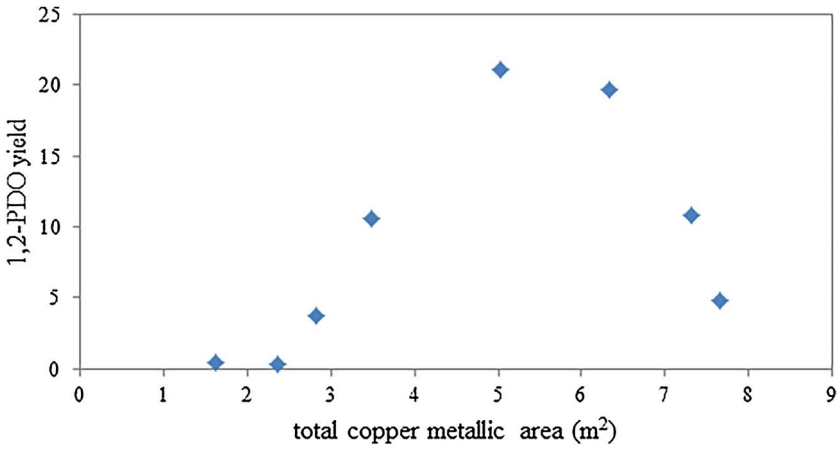

Fig. 8. Yield to 1,2-PDO vs. total copper metallic area, for CuO(x)Al catalysts.

dependence of glycerol conversion with copper loading is similar to the one observed for metallic area per gram of copper with copper loading. A change in the slope of increment of glycerol conversion vs. CuO loading is observed for catalysts with CuO contents between 10 wt% and 15 wt%. This change in the dependence of glycerol conversion is again associated with the segregation of CuO phase in the catalysts with high copper loading.

Yields to acetol, 1,2-PDO, ethylenglycol and 1,3-PDO as a function of copper loading are presented in Fig. 7. Acetol yield continuously increases with copper loading, reaching values around 83% for CuO (30)Al catalyst. This yield presented a dependence with copper loading similar to the one observed for copper metallic area, and for glycerol conversion. The yield to 1,2-PDO presents a maximum with CuO loading, for contents around 15 wt% and 20 wt%; with yields values of 21%. The ethylene glycol yield is constant independently of copper loading; then it is proposed that ethylene glycol is produced only from glycerol, by a parallel route in agreement with previous reports [19,22]. The yield to 1,3-PDO is low for all the copper loadings considered, indicating that its production is insignificant under the studied reaction conditions. In addition, it is important to point out that no gaseous products were detected during the activity measurements.

The highest yield to 1,2-PDO, was obtained with CuO(15)Al catalysts with a glycerol conversion of 74.5%. The low yields to 1,2-PDO obtained in the present study might be improved if higher residence times are employed.

The yield to 1,2-PDO vs total copper metallic area is shown in Fig. 8. The yield to 1,2-PDO has a no-monotonic dependence on metal total metallic area, reaching the maximum yield for metallic areas of 5.0-6.3 m^2 corresponding to the catalyst with a copper loading between 15 wt% and 20 wt%. Therefore, it is possible to conclude that in order to produce 1,2-PDO it is necessary the presence of metallic copper from a CuO phase highly dispersed; since the catalysts with the lower copper loading (3 wt% and 5 wt%) did not produced 1,2-PDO. Finally, it was proved that the maximum yield to 1,2-PDO is related to an optimum copper loading. For CuO loadings higher than 15 wt%, the growth of bulk-CuO crystalline particles resulted detrimental to the production of 1,2-PDO.

4. Conclusions

Regarding the textural properties of the catalysts with different copper loadings, it is evident that the mesoporous structure is accesible in a wide range of copper concentrations and high BET surface area values were maintained until CuO loadings around 7 wt%. With the incorporation of high copper contents to the alumina matrix some pore blockage might. Based on TPR profiles different copper phases were formed, which were identified as: highly dispersed CuO with strong interaction with alumina, bulk-CuO and eventually copper aluminate. The segregation of bulk-CuO segregation is significant for catalysts with copper content equal or higher than 15 wt%, while PXRD inspection confirms this only for loadings of 25 wt% or higher.

The copper phases presented in the catalysts had great influence on the metallic area and dispersion; those catalysts with higher copper loading and therefore higher copper segregation presented the lower values of metallic area and dispersion. Moreover the behavior of both, metallic area per gram of copper and metallic dispersion, with copper loading has a different dependence associated to the segregation of CuO phase.

It has been proved that the yield to 1,2-PDO has a no monotonic dependence on total metallic area. In this sense, it could be concluded that in order to produce 1,2-PDO it is necessary the presence of highly dispersed CuO phase. Besides, in order to maximize 1,2-PDO production the existence of an optimum copper loading was proved; since the highest copper contents favored the growth of bulk-CuO crystalline particles which was detrimental to the formation of 1,2-PDO.

Finally, it is important to note that a maximum yield to 1,2-PDO around 21% with a glycerol conversion of 74.5% was obtained with catalysts CuO(15)Al and CuO(20)Al; which is a promising result considering that these values might be improved at higher residence times.

Acknowledgments

Authors would like to acknowledge UBA (UBACYT 2014-2017 398BA) and CONICET (PIP 0436 2012) for the financial support.

References

[1] B. Katryniok, S. Paul, F. Dumeignil, ACS Catal. 3 (2013) 1819–1834.
[2] http://www.energia.gob.ar/contenidos/verpagina.php?idpagina=4008
[3] M. Pagliaro, Angew. Chem. Int. Ed. 46 (2007) 4434–4440.
[4] D. Sun, Y. Yamada, S. Sato, W. Ueda, Appl. Catal. B: Environ. 193 (2016) 75–92.
[5] J. Chaminand, Green Chem. 6 (2004) 359–361.
[6] M.A. Dasari, P. Kiatsimkul, W. Sutterlin, G. Suppes, Appl. Catal. A: Gen. 281 (2005) 225–231.
[7] Y. Kusunoki, Catal. Commun. 6 (2005) 645–649.
[8] S. Sato, M. Akiyama, R. Takahashi, T. Hara, K. Iniu, M. Yokota, Appl. Catal. A: Gen. 347 (2008) 186–191.
[9] E.S. Vasiliadou, A.A. Lemonidou, Appl. Catal. A: Gen. 396 (2011) 177–185.
[10] A. Bienholz, Appl. Catal. A: Gen. 391 (2011) 153–157.
[11] C. Montassier, Studies Surf. Sci. Catal. 41 (1988) 165–170.
[12] C. Montassier, Appl. Catal. A: Gen. 121 (1995) 231–244.
[13] L. Huang, J. Chem. Technol. Biotechnol. 83 (2008) 1670–1675.
[14] S. Sato, M. Akiyama, K. Inui, M. Yokota, Chem. Lett. 38 (2009) 560–569.
[15] M. Akiyama, S. Sato, R. Takahashi, K. Inui, M. Yokota, Appl. Catal. A: Gen. 371 (2009) 60–66.
[16] Z. Yuan, J. Wang, L. Wang, W. Xie, P. Chen, Z. Hou, X. Zheng, Biores. Technol. 101 (2010) 7088–7092.
[17] Y. Wang, J. Zhou, X. Guo, RSC Adv. 5 (2015) 74611–74628.
[18] L. Guo, J. Zhou, J. Mao, X. Guo, S. Zhang, Appl. Catal. A: Gen. 367 (2009) 93–98.
[19] I. Gandarias, P.L. Arias, J. Requies, M.B. Guemez, J.L.G. Fierro, Appl. Catal. B: Environ. 97 (2010) 248–256.
[20] J. Feng, W. Xiang, B. Xu, W. Jiang, J. Wang, H. Chen, Catal. Commun. 46 (2014)

98–102.
[21] C. Chiu, A. Tekeei, J. Ronco, M. Banks, G. Suppes, Ind. Chem. Eng. Res. 47 (2008) 6878–6884.
[22] C. Chiu, A. Tekeei, W. Sutterlin, J. Ronco, G. Suppes, AIChE J. 54 (2008) 2456–2463.
[23] F. Vila, M. Lopez Granados, M. Ojeda, J.L.G. Fierro, R. Mariscal, Catal. Today 187 (2012) 122–128.
[24] D. Sun, Y. Yamada, S. Sato, Appl. Catal. A: Gen. 475 (2014) 63–68.
[25] M.L. Dieuzeide, M. Jobbagy, N. Amadeo, Ind. Eng. Chem. Res. 55 (2016) 2527–2533.
[26] S. Zhu, X. Gao, Y. Zhu, Y. Zhu, H. Zheng, Y. Li, J. Catal. 303 (2013) 70–79.
[27] E.S. Vasiliadou, T.M. Eggenhuisen, P. Munnik, P.E. de Jongh, K.P. de Jong, A.A. Lemonidou, Appl. Catal. B: Environ. 145 (2014) 108–119.
[28] Y. Feng, Chem. Eng. J. 168 (2011) 403–412.
[29] M. Balaraju, V. Rekha, P.S. Sai Prasad, R.B.N. Prasad, N. Lingaiah, Catal. Lett 126 (2008) 119–124.
[30] Q. Yuan, A.X. Ying, C. Luo, L.D. Sun, Y.W. Zhang, W.T. Duan, H.C. Liu, C.H. Yan, J. Am. Chem. Soc 130 (2008) 3465–3472.
[31] S.M. Morris, P.F. Fulvio, M. Jaroniec, J. Am. Chem. Soc. 130 (2008) 15210–15216.
[32] Q. Yuan, H.H. Duan, L.L. Li, Z.X. Li, W.T. Duan, L.S. Zhang, W.G. Song, C.H. Yan, Adv. Mater. 22 (2010) 1475–1478.
[33] W.Q. Cai, J.G. Yu, C. Anand, A. Vinu, M. Jaroniec, Chem. Mater. 23 (2011) 1147–1157.
[34] H. Jiang, H. Bongard, W. Schmidt, F. Schüth, Microporous Mesoporous Mater. 164 (2012) 3–8.
[35] A. Patel, P. Shukla, J. Chen, T.E. Rufford, S. Wang, V. Rudolph, Z. Zhu, Chem. Eng. Res. Des. 101 (2015) 27–43.
[36] H. Ham, J. Kim, S.J. Cho, J.H. Choi, D.J. Moon, J.W. Bae, ACS Catal. 6 (2016) 5629–5640.
[37] S. Sato, R. Takahashi, T. Sodesawa, K. Yuma, Y. Obata, J. Catal. 196 (2000) 195–199.
[38] A. Gervasini, S. Bennici, Appl. Catal. A: Gen. 281 (2005) 199–205.
[39] M. Kruk, M. Jaroniec, Chem. Mater. 13 (2001) 3169–3183.
[40] S. Valange, A. Derouault, J. Barrault, Z. Gabelica, J. Mol. Catal. A: Chem. 228 (2005) 255–266.
[41] W. Dow, Y. Wang, T. Huang, Appl. Catal. A: Gen. 190 (2000) 25–34.
[42] J.Y. Kim, J.A. Rodriguez, J.C. Hanson, A.I. Frenkel, P.L. Lee, J. Am. Chem. Soc. 125 (2003) 10684–10692.